ANIMAL ROBOTS

A robotic honeycomb for interaction with a honeybee colony

Rafael Barmak[1]†, Martin Stefanec[2]†, Daniel N. Hofstadler[2], Louis Piotet[1], Stefan Schönwetter-Fuchs-Schistek[2], Francesco Mondada[1], Thomas Schmickl[2], Rob Mills[1]*

Robotic technologies have shown the capability to interact with living organisms and even to form integrated mixed societies composed of living and artificial agents. Biocompatible robots, incorporating sensing and actuation capable of generating and responding to relevant stimuli, can be a tool to study collective behaviors previously unattainable with traditional techniques. To investigate collective behaviors of the western honeybee (*Apis mellifera*), we designed a robotic system capable of observing and modulating the bee cluster using an array of thermal sensors and actuators. We initially integrated the system into a beehive populated with about 4000 bees for several months. The robotic system was able to observe the colony by continuously collecting spatiotemporal thermal profiles of the winter cluster. Furthermore, we found that our robotic device reliably modulated the superorganism's response to dynamic thermal stimulation, influencing its spatiotemporal reorganization. In addition, after identifying the thermal collapse of a colony, we used the robotic system in a "life-support" mode via its thermal actuators. Ultimately, we demonstrated a robotic device capable of autonomous closed-loop interaction with a cluster comprising thousands of individual bees. Such biohybrid societies open the door to investigation of collective behaviors that necessitate observing and interacting with the animals within a complete social context, as well as for potential applications in augmenting the survivability of these pollinators crucial to our ecosystems and our food supply.

INTRODUCTION

Honeybees, like wasps, ants, and other social insects, establish large self-organizing colonies, often interpreted as being self-regulating "superorganisms" (*1*–*4*). These superorganisms are important stabilizers of ecosystems and are thus considered to be "keystone species" (*5*, *6*). For example, honeybee colonies' ecological effect through pollination service by foraging is substantial for terrestrial ecosystems (*7*, *8*). Honeybees are the most important eusocial pollinators (*9*) and hence crucial for our food supply (*10*, *11*). In these ways, honeybees and their influence on ecosystems are a vital component for achieving the United Nations Sustainable Development Goals (SDGs) (*8*, *12*), especially SDG 2 (zero hunger) and SDG 15 (life on land). However, multiple anthropogenic stressors currently endanger honeybee populations (*13*, *14*). Winter is the most critical season, when a high fraction of colonies die (*15*–*17*). During this period, a colony's objective shifts from growth and reproduction to survival, via the formation of a thermoregulated cluster (*18*). Although collective thermoregulation of honeybees during the summer is relatively well understood, less is known about how they respond to dynamic conditions during winter (*19*, *20*).

Interactive robotics is an approach to studying animal behavior (*21*–*24*) whereby robotic systems generate artificial stimuli enabling investigation of how individual or groups of animals respond. This brings potential advantages of automating experimentation (*25*), presentation of complex sequences of stimuli (*26*, *27*), and stimuli that are adapted according to animals' responses in a closed loop (*28*, *29*), potentially yielding a biohybrid society (*30*). But the approach is not without challenges. Developing such a system starts with identifying a suitable interaction pathway (*31*) such that the artificial agent is accepted by living animals. Therefore, important design goals include the need for minimal disruption to the natural behaviors (when not intentionally exerting influence), robustness to the animals and their local environments, and reliability for time scales spanning the behaviors of interest. Moreover, understanding the dynamics of specific behaviors may require multiple interactions (*26*, *27*) or interacting with multiple individuals (*30*, *32*). The latter point is especially pertinent in the study of collective behaviors expressed by honeybees in winter, which involves coordination of behaviors of thousands of animals (*33*) over periods of several months (*18*). Overcoming these challenges in developing robotics to modulate self-regulatory collective behaviors within a host bee colony could ultimately form a biohybrid superorganism. The robotic component of such a hybrid superorganism would enable us to better understand and to interact with honeybee collective dynamics from within their society, even in challenging situations, such as during the winter period.

Here, we present such a robotic device that thermally interacts with an entire colony of honeybees (*Apis mellifera carnica* Pollmann) comprising thousands of worker bees and a healthy queen (Fig. 1 and Movie 1). We conducted experiments with this robotic system by observing and interacting with three colonies for several months during the 2020 and 2021 winter seasons. In a perturbation experiment, we demonstrated that the robotic device systematically controlled the location of the winter cluster. Moreover, through the sensor array, we detected the thermal collapse of a weakened colony that fell into a chill-coma state (*34*), and using thermal actuators, we were able to "resuscitate" the colony out of this unviable state, consequently extending its life. In another perturbation experiment, the robotic system autonomously measured colony reorganizations and

[1]Mobile Robotic Systems Group, École Polytechnique Fédérale de Lausanne, Lausanne, Switzerland. [2]Artificial Life Lab, Department of Zoology, Institute of Biology, University of Graz, Graz, Austria.
*Corresponding author. Email: rob.mills@epfl.ch
†These authors contributed equally to this work.

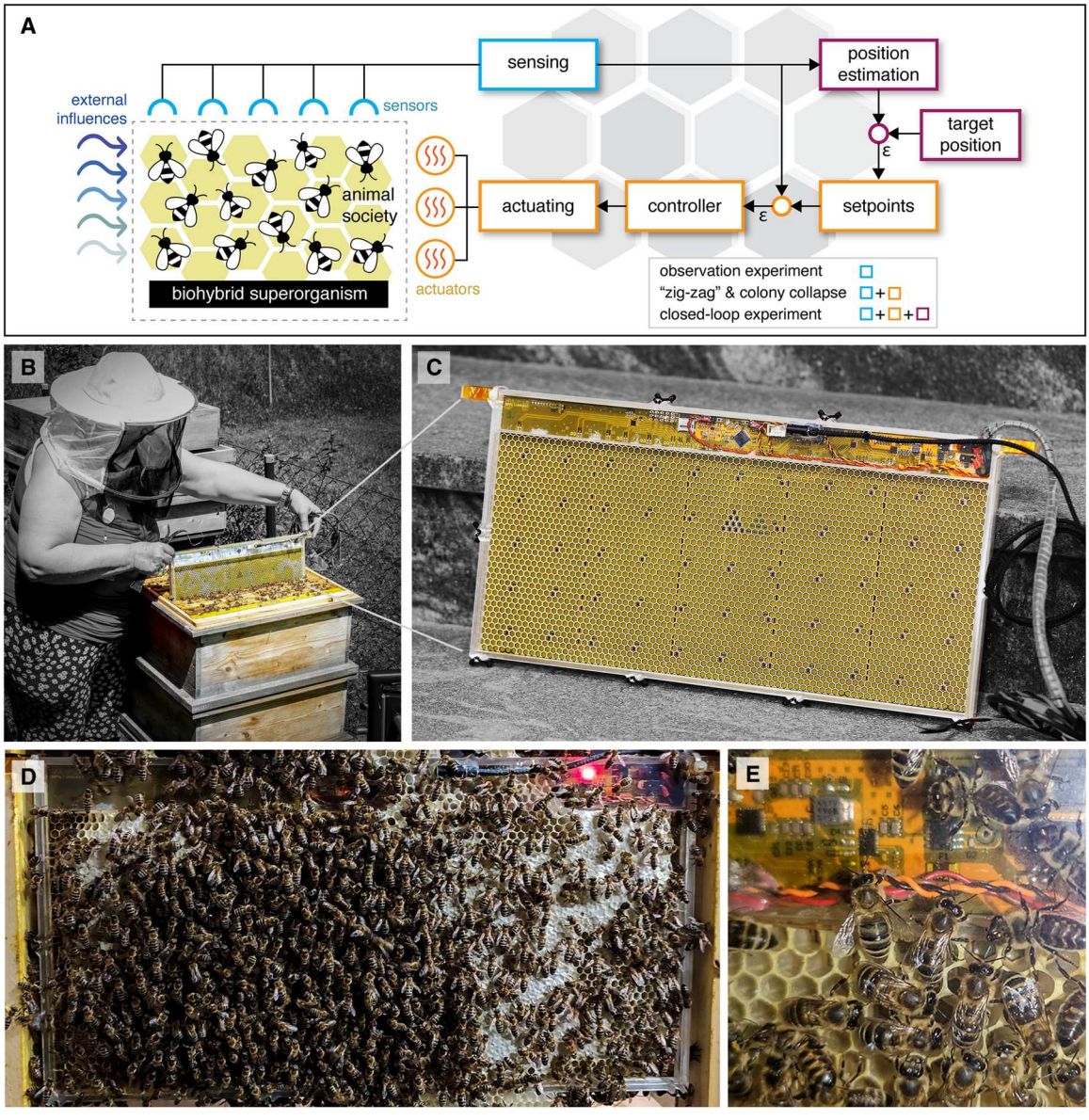

Fig. 1. A robotic system designed to conform to scientific and agricultural beehives. (**A**) Honeybee/robotic biohybrid superorganism overview, including the regimes used in the experiments to control environmental (thermal) and behavioral (colony position) variables. (**B**) A photograph of a beekeeper performing a field verification of the robotic device, fitting it into a standard box hive used in agricultural beekeeping. (**C**) A photograph of the assembled robotic system ready to be installed into a hive. In (B) and (C), the beekeeper and the background were made black and white to emphasize the robotic device. (**D**) The robotic system operating in an observation hive. (**E**) A close-up image showing complete wax cells and bees close to the electronics bay, which is enclosed within transparent acrylic.

reacted by generating new thermal stimuli to repeatedly reposition the cluster, thereby demonstrating a closed-loop animal-robot interaction. We validated, in an observation hive (see fig. S5C), that identification of colony parameters and modulation of winter cluster organization were feasible with our embedded biocompatible robotic system. Our system creates a pathway for field applications with conventional beehives, within which measuring colony parameters and applying appropriate actuation are challenging. Such application may expand our knowledge of thermally mediated collective behaviors and emergent patterns in these pollinators vital to our ecosystems, to our agriculture, and consequently to our food security.

One environmental factor that highly influences honeybees is temperature. Accordingly, they exhibit diverse thermoregulatory strategies, building on individual (*35*, *36*) and social (*37*–*39*) mechanisms. For example, they tightly regulate the thermal microclimates to raise their young (*40*) and reduce high temperatures throughout their hives (*41*, *42*) and at localized hotspots (*43*). Moreover, honeybees respond to low temperatures by endothermic heat generation (*44*), especially within the winter clustering behavior (*45*), when a colony forms a dynamic self-regulating aggregate of thousands of bees that behaves like one single larger organism, affording survival in cold climates. Recognizing the bees′ sensitivity to temperature, prior research developed robotics that interacted with

Movie 1. Overview of robotic system to interact with a honeybee colony.

small groups of young honeybees, successfully modulating their behaviors with localized thermal stimuli under laboratory conditions (*46*–*48*). Therefore, a thermal pathway offers a promising candidate for a robotic platform to interact with entire colonies.

Our goal is to leverage robotic capabilities in scientific studies of honeybee collective dynamics, specifically by means of robotic interactions that can provoke the animals' responses through modulation of localized thermal fields inside the hive. Understanding the emergent collective behaviors of colonies exposed to cold periods is difficult. This paper presents a robotic system that interacts with an overwintering superorganism that can be embedded into scientific and conventional hives. The robotic system demonstrated the ability to observe and quantify the thermal profiles of winter clusters during healthy and collapsing states. We also demonstrated the capacity to regulate colony-level activity by influencing the movement of the bee aggregation in multiple colonies. The robotic system presented here has the capability to integrate into a honeybee colony and the potential to investigate their diverse collective thermoregulatory behaviors.

RESULTS

To evaluate the robotic system's ability to form a biohybrid society with a honeybee colony, we installed the system inside an observation hive populated with a queenright colony with about 4000 bees (colony A). Hives were situated in the Honeybee Field Laboratory in Graz (HFLG), Austria (see Materials and Methods). First, we used the system to observe the natural activity of the colony (without the injection of any modulatory stimulus) to verify the capacity of the collected data to reveal specific collective behavior patterns. Second, we performed an experiment to assess whether the thermal actuators were able to emit meaningful stimuli to interact with the colony, to modulate its position in the hive. Third, we identified the thermal collapse of a colony using the sensory system and reported our efforts to revive the colony using thermal actuators. Last, we tested the robotic system in an autonomous mode where it estimated and modulated the position of the colony.

Observing collective behaviors with a robotic system

To verify the system's capacity to monitor honeybee's thermoregulatory collective behavior, we used the system to observe a colony for 1 week in the 2020/2021 winter season, when all members of the colony tend to form a cohesive winter cluster. These observations (photographs and thermal data) are shown in movie S1. When temperatures around the hive dropped below T_{amb} = 11.2°C, we observed the characteristic ellipsoidal shape of the winter cluster (*49*), with bees oriented inward and aligned with the temperature gradient (Fig. 2A) (*50*). The characteristic spatial organization of the winter cluster (*44*, *51*) is reflected in the thermal data collected by our system (Fig. 2B and movie S1).

Temporal dynamics of a winter colony

Honeybee thermal behaviors have differing temporal characteristics. Some have short durations [for example, individual bees heating brood cells (*40*)], whereas others can span a period of months [such as winter clustering (*49*) and collective brood nest thermoregulation (*52*)]. Hence, for a robotic system to integrate with a hosting colony, it must be able to properly sample the temporal evolution of the behaviors of interest.

To test whether the robotic system was able to capture the temporal dynamics of the winter cluster, we computed the cluster's location and corresponding temperature values. We used computer vision to calculate the cluster's location using images and calculated the temperatures defining the cluster's outer edge T_{mantle}, the core contour T_{core}, and the core centroid T_{cen} in 10-min intervals (n = 1008). The temperatures on the perimeter of the winter cluster T_{mantle} (Fig. 3A, yellow) followed the ambient temperature patterns T_{amb} (Fig. 3A, blue; Spearman correlation ρ_s = 0.82, lag of 0.34

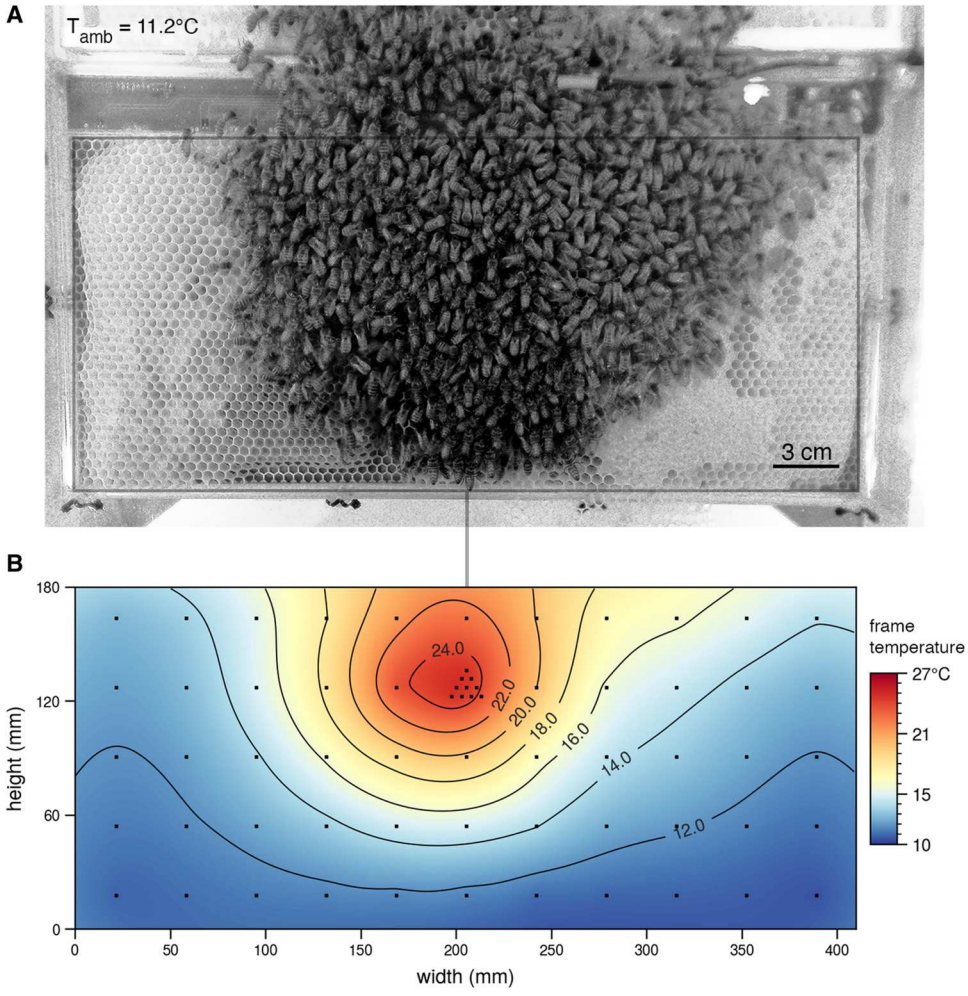

Fig. 2. A robotic system capable of observing collective thermoregulatory behaviors. (**A**) A photograph of a broodless bee colony displaying a winter cluster formation. (**B**) The associated thermal field generated by the linear interpolation of the data from an array of 64 temperature sensors (black markers).

hours, $P < 0.001$) with a median offset of +3.8°C, suggesting that the colony adjusted its structure to remain inside a safe thermal range (*49*, *53*). When bees' body temperatures drop below T_{chill} = 10°C (Fig. 3A, black dotted line), they fall into a comatose state, or "chill-coma," where they can no longer move or self-heat (*34*, *36*). Furthermore, the similarity in the slope values of the first-order regressions between T_{mantle} and T_{amb} against T_{ext}, rendering parallel curves (Fig. 3B, yellow and blue), reinforces the observation that the cluster adjusted to ambient temperatures (*53*, *54*). The mantle is where most ectothermic bees are located (*51*), and the cluster core hosts the majority of the endothermic bees (*44*). The border region between the core and the mantle displayed fast-changing dynamics (Fig. 3A, orange) but little sensitivity (that is, decoupling) to changes in ambient temperature (low slope in Fig. 3B, orange). The core centroid temperature T_{cen} (Fig. 3A, red), at the positions calculated from processed images, closely follows the maximum temperature of the thermal field (Fig. 3A, purple; $\rho_s = 0.98$, lag of 0.17 hours, $P < 0.001$). T_{cen} is more sensitive to external variations than T_{mantle} (observe the regression line slopes for T_{cen} and T_{mantle} in Fig. 3B).

Ambient temperature has a large influence on how a colony behaves, therefore making it an essential variable to record. During the observation period, the external temperature T_{ext} ranged between −7.1° and 7.1°C (Fig. 3A, dark blue) and remained below the bee chill-coma threshold T_{chill} = 10°C (Fig. 3A, black dotted line). The ambient temperature inside the field laboratory T_{amb} ranged from 8.0° to 17.1°C (Fig. 3A, blue) and followed the changes in external temperature (Fig. 3B, dark gray; $\rho_s = 0.96$, lag of 2.0 hours, $P < 0.001$) but with a positive median offset of 11.2°C. Inside the hive, the minimum temperatures measured in the populated frame T_{min} (Fig. 3A, gray) were very close to the temperature surrounding the hive T_{amb} (median offset 1.0°C). Note that there were brief periods where T_{min} was lower than T_{amb}, because T_{ext} was always below T_{amb}, and cold air can flow into the hive through its entrance.

Spatial organization of a winter cluster

Winter clusters consist of thousands of bees (*55*, *56*), usually positioning themselves in thermally optimal locations, typically in the center of the hive (*49*, *54*). However, a cluster may also actively relocate itself toward honey reserves (*49*), which are needed for

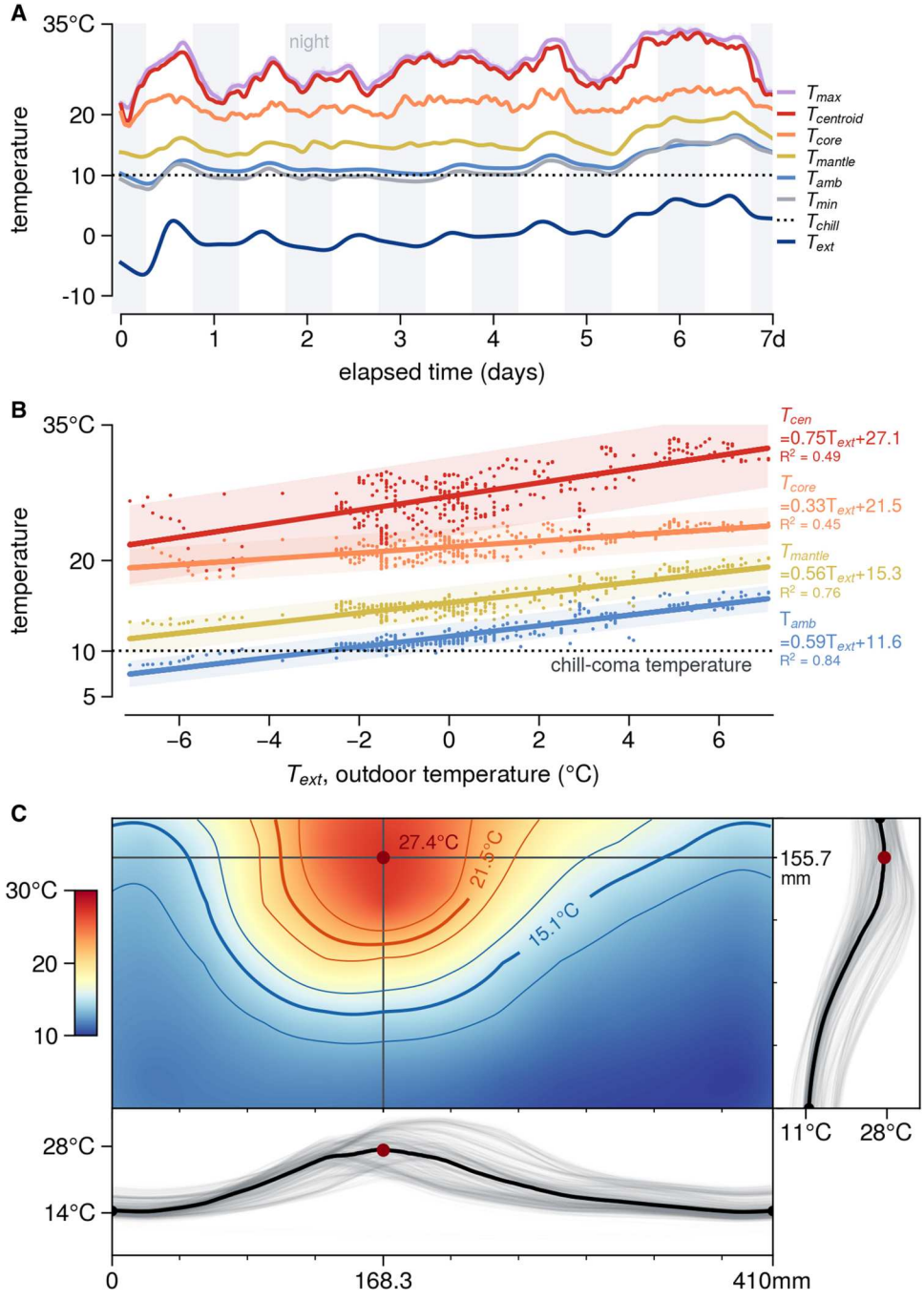

Fig. 3. Observation of the temporal and spatial dynamics of a winter cluster. (**A**) Temporal variations of different temperatures in the system. T_{cen}, T_{core}, and T_{mantle} were calculated at 10-min intervals (n = 1008), and T_{amb} and T_{ext} were sampled every 30 min (n = 335). Data were smoothed with a trend filter. (**B**) Linear least squares regressions revealing the relationship between outdoor temperature and the temperature of the HFLG, T_{amb} (blue); cluster mantle contour, T_{mantle} (yellow); core contour, T_{core} (orange); and core centroid, T_{cen} (red). Color bands represent measurements' 95% confidence interval. (**C**) Heatmap visualizing the median thermal field of the winter cluster during the observation period. Isotherms defining the outer edge of the cluster (blue) and the region of higher endothermic activity (orange) are shown. The median core centroid position is represented by a red circle. The thin lines delimit the isotherm uncertainty and are the MADs. Bottom and right depict the median thermal profiles of the horizontal and vertical transects crossing the core centroid (n = 1008).

heating. Accordingly, a small number of sensing devices at fixed locations will fail to track the moving cluster throughout a season (*57*), but a dense array of sensors enables an accurate spatial representation of the signals generated by behaviors of interest.

We calculated the median thermal field of the cluster over the observation period (Fig. 3C). This thermo-spatial distribution captures the thermal gradient characteristic of winter clusters, with higher temperatures in the core than the periphery (*44*, *49*). By overlapping the image-based contours with the measured median thermal field, we found the representative median temperatures for the outer edge of the cluster $\overline{T}_{\text{mantle}}$ = 15.09° ± 1.21°C, the core perimeter $\overline{T}_{\text{core}}$ = 21.59° ± 1.54°C, and the core centroid $\overline{T}_{\text{cen}}$ = 27.39° ± 3.03°C (Fig. 3C).

Robotic modulation of the winter cluster's position

For a robotic system to successfully integrate into an animal society, it requires the capacity not only to measure the state of the colony but also to emit relevant cues or signals to modulate behaviors of interest (*21*–*23*, *31*). The objective of the present experiment was to assess and characterize whether the thermal pathway could influence the animal collective. Specifically, we aimed to answer the question of whether the thermal cues emitted by the robotic system can affect the colony's collective position. We tested this with a perturbation experiment on colony A. We sequentially activated one of the five pairs of thermal actuators of the robotic system from one extremity of the frame to the other, creating a thermal stimulus with a zig-zag pattern (Fig. 4 and movie S2). To attract the bees toward the actuator area, we adjusted the controllers' objectives to 25°C. This setpoint was warmer than the hive's ambient temperature (the experiment started with T_{amb} = 14.1°C), serving as a cue to attract bees to the warmer zone of the actuators, but lower than usual spring/summer temperatures. This avoids inducing potentially harmful behaviors during cold periods, such as onsets of foraging or breeding. Each actuator pair was active for a fixed period of 3 days. After each stimulation period, the actuators were turned off, and the adjacent pair was enabled. This experiment lasted 51 days, with a 3-day initialization phase and 16 transitions.

To evaluate the movement of the cluster toward the thermal actuators, we computed the cluster's outer perimeter, its centroid position, and the horizontal distance of the centroid to the center of the actuator pairs (fig. S1). When the actuator pair advanced to the next location (Fig. 5A, light yellow squares), the bee cluster followed it, which can be observed by how closely the centroid of the cluster followed the heated patches (Fig. 5A, red and blue, and movie S2; Spearman correlation ρ_s = 0.96, lag of 1.1 days, $P < 0.001$). This result also shows how similar the locations of the front and back subclusters are, with one mirroring the other (ρ_s = 0.99, lag 0, $P < 0.001$).

To increase the likelihood of system acceptance by the colony, we designed the thermal actuators' controllers to allow animals to participate in the control loop (*24*). The temperature of endothermic bees was measured by sensors used in the control logic. This means that the balance of heat produced by the bees versus by the robotic agent was affected by the bees' behaviors. Consequently, instead of a constant power injection, the amount delivered was influenced by T_{amb} and the animals (Fig. 5B, yellow). During the experiment, the active thermal actuators operated at 51% of their maximum capacity (median power 0.77 ± 0.27 W, n = 34 activations, power limited to 1.5 W). All the thermal actuators dissipated

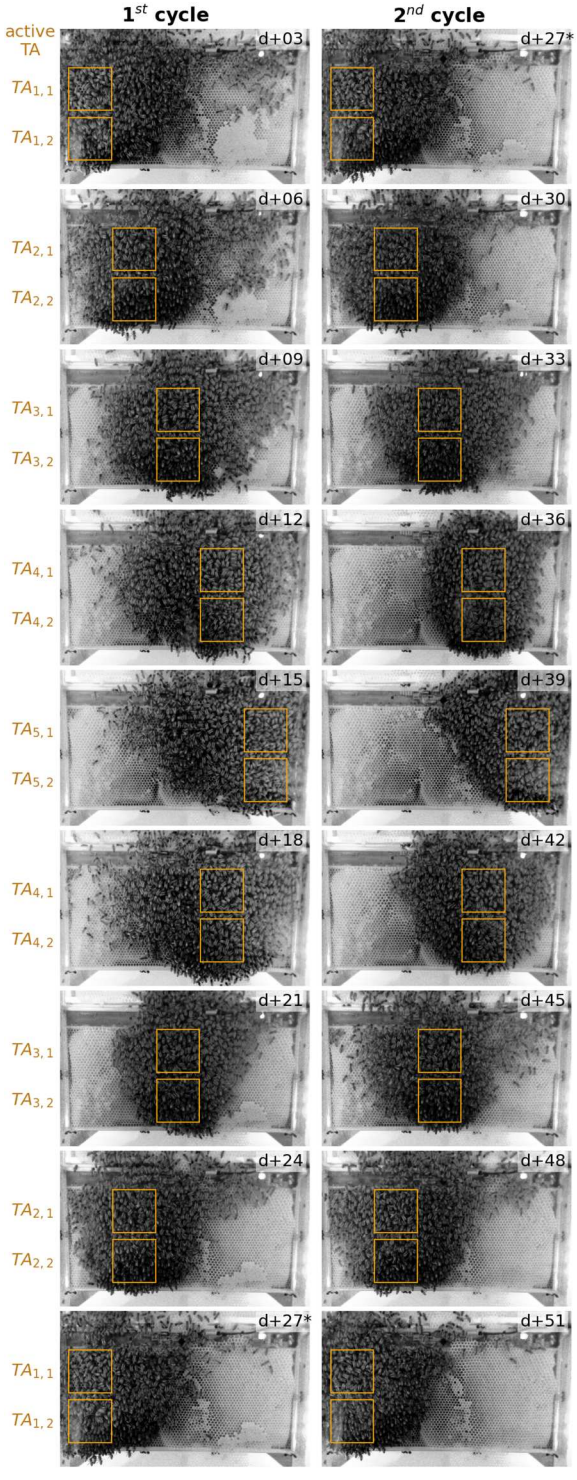

Fig. 4. Thermal stimulation to modulate the winter cluster's position. Time lapse showing the 51 days of experimentation, depicting an aggregation of bees following the thermal stimuli emitted by pairs of actuators organized in five columns (orange). Thermal actuators indexed following the convention: $TA_{\text{column, row}}$. Each frame corresponds to the end of an activation period, every 3 days, with initial day d_0 = 8 December 2020. The last image of the first cycle (d + 27, left-bottom) is duplicated as the starting image of the second cycle (right-top). Only the front side of the cluster is shown, because the back subcluster followed a similar trajectory.

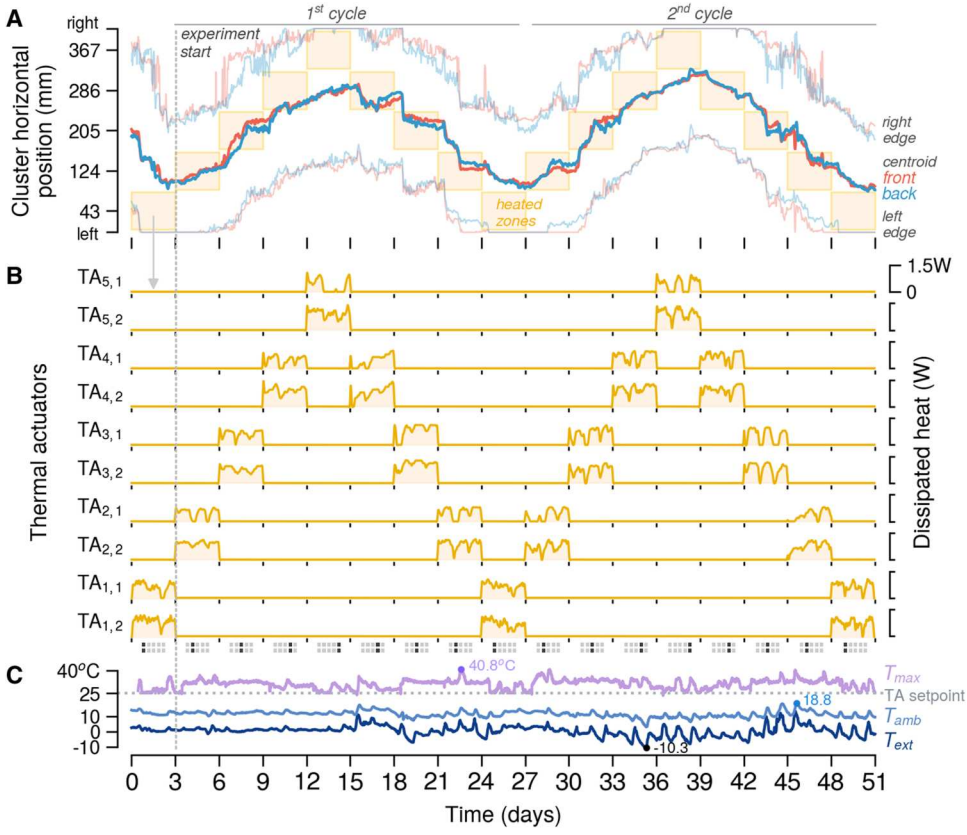

Fig. 5. The influence of the robotic system on honeybee collective position. (**A**) The change in position of the cluster with respect to thermal actuators. The horizontal centroid position and the cluster's left and right extreme positions of the back (blue) and front (red) subclusters are shown. Cluster perimeter and centroid were calculated every 30 min. (**B**) Thermal actuator activation sequence and injected power over the course of the experiment (yellow). Actuator data were sampled every 10 s and trend-filtered. (**C**) External T_{ext} (dark blue), HFLG T_{amb} (blue), and T_{max} (purple) temperatures, sampled every 30 min.

a total energy of 6.13 ± 0.59 MJ [median ± MAD (median absolute deviation)] in 51 days. We estimate this energy to correspond to about 68 g/day of honey, equivalent to 15% of the energetic demands of the colony (see Supplementary Methods for details of the derivation).

The broad temperature range observed inside the HFLG, T_{amb} from 3.1° to 18.8°C (Fig. 5C), did not impair the robotic device's capacity to modulate the colony position observed by the cohesiveness of the bee cluster (and the weak negative monotonic correlation between T_{amb} and the cluster centroid, with a peak correlation of $\rho_s = -0.26$, $P < 0.001$, over a 10-day window). When the ambient temperature increased (such as on day 45), the winter cluster expanded and was less influenced by the actuators' thermal cues, which can be seen by the higher variability in the cluster's horizontal position (Fig. 5A).

The cluster moved neither immediately nor constantly toward the new stimulus (fig. S1). Rather, it took 11.6 ± 1.5 hours to start moving (considered after the cluster center moved 5 mm from the previous position) and 15.1 ± 10.8 additional hours to enter the zone of the newly activated actuator (fig. S1A). The cluster speed increased during the night to a maximum of 9.3 cm/day (fig. S1B). The cluster could align itself with active actuators in the center of the frame but to a lesser degree at the edge of the hive (movie S2, Fig. 5A, and fig. S1C).

Winter colony collapse and robot-mediated resuscitation

Stressed or weakened colonies are more susceptible to colony collapse (*58*). No other period is more critical than winter, when a high percentage of colonies die (*15*–*17*). When temperatures drop inside the colony, bees can fall into a chill-coma that could lead to their deaths (*59*). In this state, bees can no longer self-heat, but the state is reversible if they are warmed by an external source (*34*). Inducing such a state would be unethical, but because it occurred to a colony under observation by our robotic system, we were able to test the robot-mediated augmentation of this animal society. Exploiting the sensing and modulating capabilities of the robotic device demonstrated above, we intervened in a colony identified at a critical state. During the winter of 2021/2022, a standard treatment against varroosis (*60*) was performed in an effort to strengthen colony B (spraying 3 ml of 3.5% oxalic acid). Soon after the application of oxalic acid (time t_0), the robotic device observed changes in the endothermic area ($\overline{T}_{core} > 21.5$°C, see above). About 6 hours later, the area started to shrink until it disappeared at $t_0 + 11.3$ hours (Fig. 6B), indicating that bees had stopped their endothermic activity and eventually fell into chill-coma. The decrease in endothermic activity was also evident in the maximum temperature T_{max} (Fig. 6C, orange), which displayed a declining trend a few hours after the treatment. Moreover, the recorded images revealed no visual signs of motor activity, with bees standing still (movie S3).

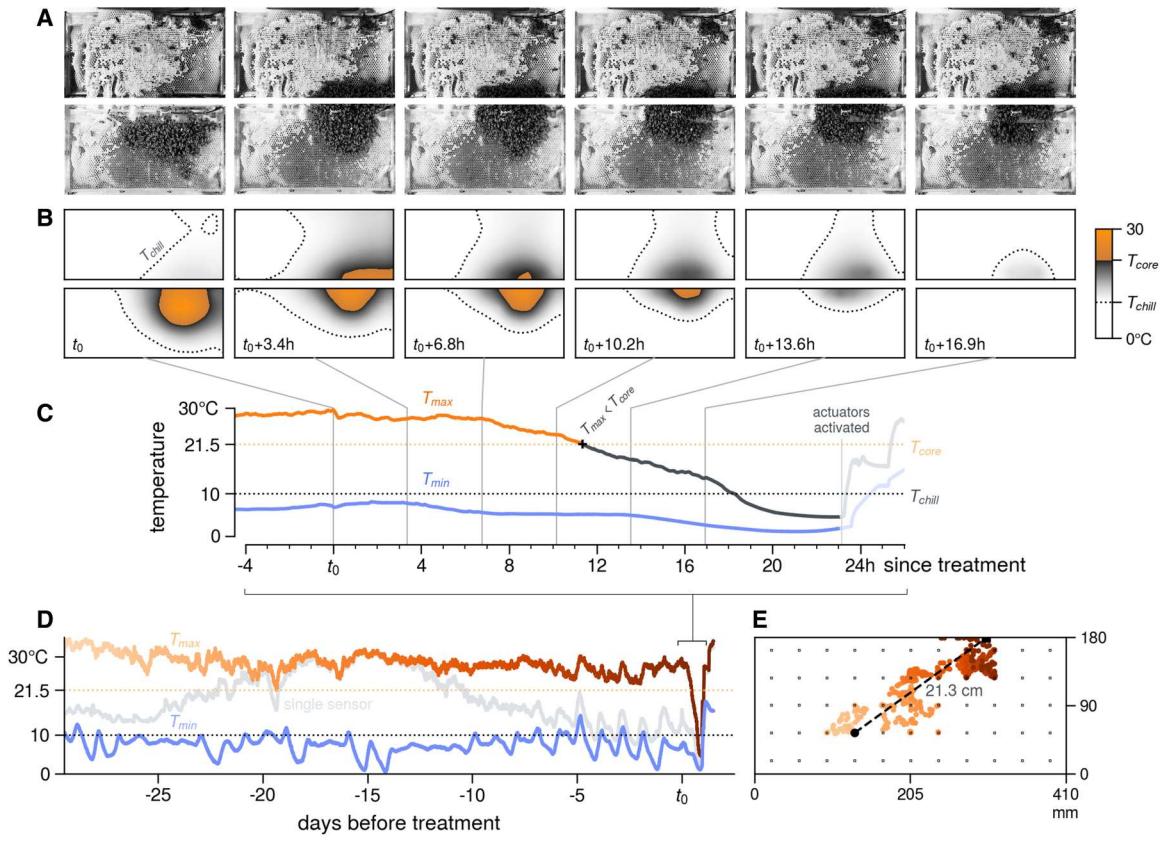

Fig. 6. The collapse of a honeybee winter colony can be detected by its thermal dynamics. (**A**) Images showing the colony during thermal collapse, at the moments indicated in (B) and (C). When the cluster falls into a chill-coma, it can maintain about the same shape of a healthy thermogenic cluster. Therefore, diagnosing a colony in a critical state by visual inspection, especially with still images, can be difficult. (**B**) Temporal evolution of the endothermic area (orange region). The black dotted line defines the isotherm at chill-coma threshold, T_{chill} = 10°C. (**C**) Time series of the minimum temperature T_{min} (blue) and maximum temperature of the frame T_{max}, which is colored orange whenever $T_{max} > \overline{T}_{core}$, implying the presence of a thermogenic core in the winter cluster. T_{max} color changed to gray when $T_{max} \leq \overline{T}_{core}$. Around t_0 + 23 hours, all thermal actuators were manually activated, causing the T_{max} and T_{min} to rise. (**D**) Evolution of the cluster's maximum temperature T_{max} over a 30-day period before t_0 (orange). The gray curve represents the temperature of a single sensor in the center of the frame, illustrating the necessity of multiple sensors. The blue curve shows T_{min}. (**E**) Spatiotemporal evolution of the point of maximum temperature in the cluster, d_{Tmax}, over a period of 30 days [time is encoded with the same colors as (D)].

About 5 hours after the robotic system indicated temperatures below the chill-coma threshold, T_{chill} = 10°C, we decided to try resuscitating the bees using the thermal actuators (Fig. 6C, faded curves). We manually applied a multistep heating procedure that reanimated the comatose bees, which allowed them to reaggregate, and then guided them using robotic modulation toward honey supplies on the opposite side of the hive. About 2 hours after activating the thermal actuators, we observed bees regaining motion, and 20 hours later, the surviving bees regrouped into a new cluster. Despite the colony not ultimately surviving (likely because of the loss of the queen), our "resuscitation effort" avoided its immediate collapse and extended its life for over 2 months (movie S3).

The robotic system showed that the winter cluster is not a static aggregation. During the 30 days before the oxalic acid treatment, the cluster's point of maximum temperature moved considerably, $d_{T\text{max}}$ = 21.3 cm (Fig. 6E). This implies that any single sensor placed inside a hive would have failed to capture the thermal signature of the cluster (Fig. 6D, gray curve). However, because our robotic devices have arrays of temperature sensors, they could accurately reveal the cluster's repositioning.

Autonomous closed-loop interaction

The synthesis of a biohybrid society relies on the capacity of living and artificial agents to interact. We aimed to test whether the robot could use its sensory information to perceive colony states and autonomously generate new stimuli in response. Therefore, we devised a perturbation experiment to attract the winter cluster to one of two designated regions, defined as zone L (left side) and zone R (right side), and composed of four thermal actuators each (movie S4). Once the system detected that the cluster's residency time within one of the target zones was longer than 12 hours, it activated the thermal actuators of the second zone with the intention to attract bees there. The robot relied solely on its thermal sensing array to estimate the cluster's position.

During a period of 16 days, colony C repeatedly responded to stimuli generated by the robotic device (Fig. 7B). Each time the system was able to find the cluster's centroid position and detect that bees were inside the selected zone (Fig. 7C, green segments), it generated a new thermal landscape. In contrast to the fixed-time regime used in the modulation experiment (Fig. 4), here, the robotic system and animals jointly defined the transitions in thermal stimuli. Specifically, the robotic system waited for the

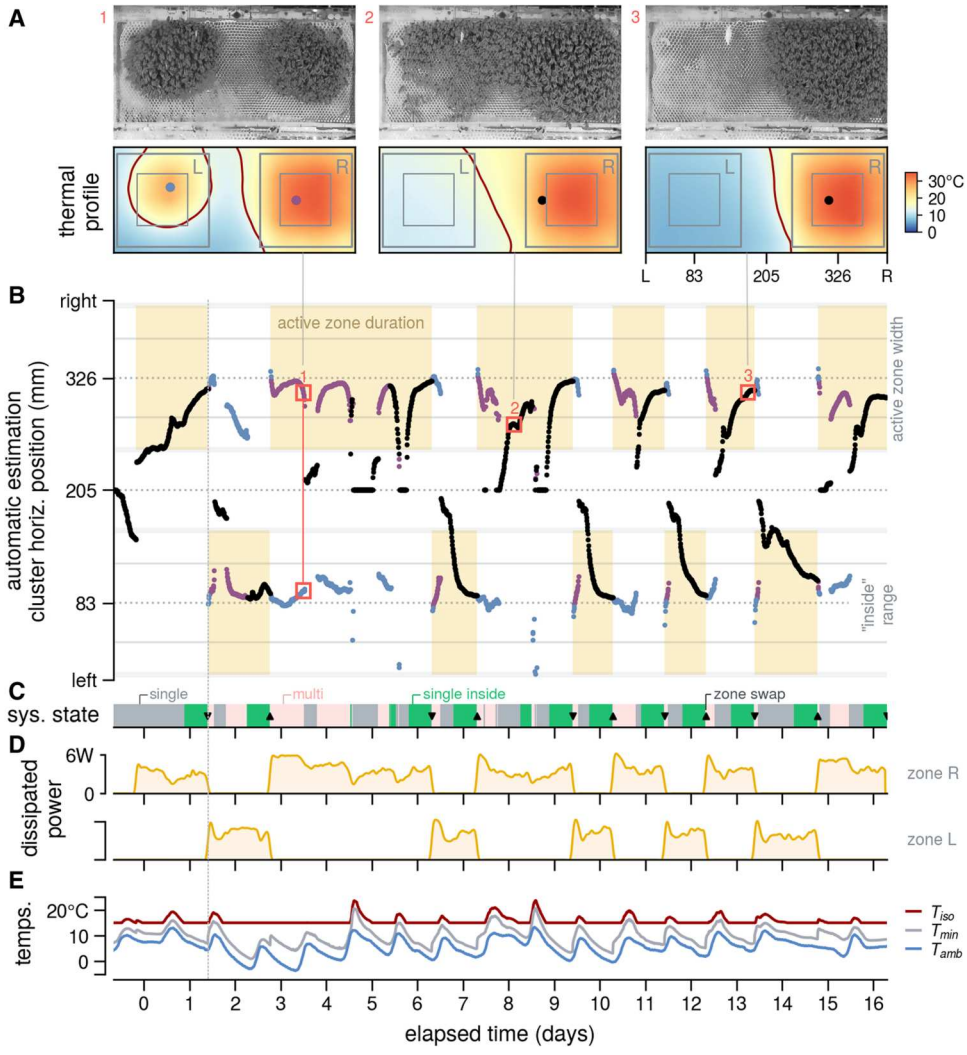

Fig. 7. Autonomous interaction between robotic agent and animal colony. (**A**) Examples of three frequent states detected by the system: (1) When the cluster was split in two or it was far from the active zone, two thermal hotspots were observed (the bee cluster and the actuators). This condition does not allow the robotic system to distinguish the true location of the winter cluster. (2) When just one maximum was defined but its centroid was outside the active zone. (3) When the detected contour was inside the active zone. (**B**) Time series of the estimated position of the cluster in response to the activated thermal zone (orange patches). Single centroids are depicted by black markers. When two centroids were estimated, their positions are represented by purple and blue markers. (**C**) Autonomously identified states: cluster outside (gray) or inside (green) new stimulated zone or undefined colony position where multiple centroids were found (pink). (**D**) Total dissipated power by the four thermal actuators of each zone (orange curves). (**E**) Relevant temperatures for the biohybrid interaction: T_{iso} (red) is computed from T_{min} (gray) that serves as a proxy for T_{amb} (blue).

animals to adjust to the stimulus, which had a variable timespan as expected within natural societies. The median active zone residency time was 29.8 ± 9.4 hours (range, 21 to 85 hours; n = 10), with a residency time at zone R, 36.4 ± 16.2 hours (n = 5), slightly longer than zone L, 23.6 ± 3.9 hours (n = 5). Together, these results demonstrate that our robotic device was able to systematically modulate colony position autonomously, based on successful perception of the animals and effective stimulus generation.

DISCUSSION

Our results imply that robotic systems are capable of integrating and interacting with full-sized honeybee colonies. The presented robotic device could observe the thermal characteristics of the winter cluster (movie S1), consistent with prior observations (*44*, *49*, *54*), with high temporal and spatial resolution. Moreover, it was able to measure the thermal profile of a collapsing colony, providing potentially valuable data for future predictive systems of colony health. Our study yields two key results: first, the robotic platform's ability to systematically reposition the cluster, formed by thousands of bees, following a predefined pattern over 51 days (Fig. 1 and movie S2); second, using the robotic system in an autonomous mode, we successfully demonstrated that it was capable of perceiving the animals' position and consistently influencing their movement for 10 transitions over 16 days (movie S4). Key properties of the presented system are its biocompatibility, dense array of sensors, and thermal actuation in close proximity to the cluster. These characteristics enabled the robotic system to successfully interact with

intact honeybee colonies over substantial periods, including the control of the movement of a large number of animals.

The proximate mechanisms of winter cluster thermoregulation, including displacement of the bees, are still unresolved research questions. Stabentheiner *et al.* (*44*) identified competing hypotheses that differ with regard to the mechanisms essential to explain the cluster organization. Studies using in silico models addressing the within-cluster self-regulation (*61*–*65*) and formation (*63*) have been based and validated on data from experiments with entire honeybee clusters subjected to various uniform ambient temperatures (*44*, *49*, *66*). Our system can generate nonuniform thermal stimuli that can be located inside or outside of the cluster and can move over time. These stimuli offer possibilities for experimentation to better understand behavioral mechanisms and thus stimulate refined modeling. For instance, our results showed several observations inconsistent with some assumptions made in state-of-the-art models, such as individual positive thermotaxis of bees (temperature gradient climbing) (*61*–*65*). Specifically, the cluster was able to sense a localized thermal cue that was outside of its own perimeter. For the cluster to relocate to such newly appearing cues, the new area was only reachable by traversing a local temperature minimum in several cases (such as in Fig. 7A). These observations reject a hypothesis of individual thermotaxis toward a preferendum. New models may incorporate a method of representing bees moving outside of the cluster, such as through an additional state that relaxes the need for thermotaxis to allow random exploration. A model including this feature may be able to reflect the local minimum traversal dynamics observed, although care would be needed to avoid undermining the existing ability to maintain a cluster.

Although our system was developed to investigate collective behaviors, we can nonetheless envisage some immediate applications in supporting the colony. For example, the robot's sensing and actuating capabilities allowed us to manually execute a "resuscitation maneuver" on a colony under observation. This action prevented the immediate death of the colony and allowed the remaining bees to regain mobility and to reaggregate into a single compact cluster. Because the rescuing heating was not switched on until about 6 hours after the bees fell into a chill-coma (when $T_{max} < T_{chill}$), a large number of bees and the queen were lost, removing the colony's chance of repopulating. Ultimately, the number of surviving bees was already too low to sustain the colony until the foraging season commenced in the next spring. Despite the colony's ultimate demise, the robotic device managed to keep the bees alive for over 2 months. This gives hope that future autonomous colony health monitors will enable the application of supportive heating at early stages of the collapse, increasing the probability of a full recovery. Further investigation is required to understand the effects of prolonged heat injection on aspects including the ratio of endothermic (active) to ectothermic (passive) bees and the colony metabolic consumption (*67*). Such an understanding should inform the development of efficient strategies for robotic intervention. More generally, the observational and modulatory capacity of such robotic systems, tightly integrated into a hosting honeybee colony, could be beneficial in several ways. Observations of the animal society can contribute to designing data-based health monitoring systems (*68*, *69*). Modulation systems could be used in automating heat treatments against varroa (*70*) or to actively intervene in a distressed colony to try to revert its collapse. For instance, during winter, colonies can die from starvation despite honey stores remaining in unreachable cold regions (*51*), and an array of embedded thermal actuators could provide safe passages to make them accessible. Despite the single instance of the presented robotic intervention, temporarily reverting the fate of a collapsing colony, this result emphasizes how robotically enhanced organisms could be more resilient to challenging habitats.

Observation hives provide an invaluable way to study behaviors from intact colonies, which interact with their natural ecosystems, in otherwise obscured regions of a hive (*39*, *71*). However, they bring some drawbacks, including an increased risk of luminous contamination inside the hive and reduced thermal isolation when compared with tree trunks or box hives (*18*, *72*). Furthermore, these hives limit populations to 4000 to 20,000 individuals (*18*). Moreover, in observation hives, frames are usually stacked vertically instead of parallel to each other, constraining bees to form more disk-like clusters during cold periods. However, our system is compatible with box hives (Fig. 1B), where multiple robotic devices could be placed parallel to each other. We see an opportunity for experiments with colonies that adopt more diverse topologies, including those seen in apiculture, as well as in summer seasons, during which honeybees exhibit various other collective behaviors. Application in field scenarios could ultimately support an important keystone species on a large scale, because one colony can forage and pollinate more than 100 km^2 (bees fly up to 14 km) (*18*). This way, such autonomous robotic systems can also contribute to ecosystem stabilization and agricultural improvements.

MATERIALS AND METHODS

Robotic system design

The robotic system comprises three submodules: the system orchestration and data processing, the thermal sensing, and the thermal actuation. For orchestrating the execution of low-level controls and high-level communication with external users and devices, we used an ARM Cortex-M4 32-bit microcontroller unit (MCU, STMicrosystems STM32F405). In the MCU, a real-time operating system (ChibiOS v19.1) provided a multithread scheduler to run applications in a single-core processor. To make available an external interface to data, code, and commands between the robotic device and users or devices outside the hive, we made a USB communication channel accessible (fig. S5A).

Thermal sensing

We selected a small (2.0 mm by 2.0 mm by 0.8 mm) silicon-based temperature sensor (TI TMP117) that fit within inside a honeycomb cell (preliminary trials with larger sensors caused bees to avoid the area nearby). This sensor returned a 16-bit temperature value with a resolution of 7.8125×10^{-3}°C and can operate in the range of −20° to 50°C with an accuracy smaller than ±0.1°C. The robotic device was equipped with 55 temperature sensors arranged in a 5 by 11 array with vertical and horizontal spacings of 36.4 mm and 36.8 mm, respectively (fig. S5B). In addition, to allow the investigation of finer details of thermal fields, we positioned a nine-sensor high-density patch at the central axis of the frame (fig. S5B), bringing the total number of sensors to 64. Because these sensors use an I_2C digital communication bus, with the possibility of four different identification addresses, a circuit with two 8-channel multiplexers (TI TCA9548A) was devised to connect all 64 sensors to a single I_2C port in the MCU (fig. S5A).

Thermal actuation

Bees adjust the metabolic intensity of specific thermogenic activities to the hive microclimate and social conditions (such as winter clustering and brood care). In general, the average maximum metabolic rate is about 115 W/kg at 10°C and decreases at higher temperatures (*35*, *45*, *55*, *73*). To allow our system to generate thermal cues with intensities similar to natural behaviors, we distributed 10 thermal actuators (2 by 5 array), in the bee-occupied area of the robotic device, with a total dissipation capacity of 158 W using a 12-V supply, similar to the peak metabolic rate of a 1-kg honeybee colony [~7700 bees (*74*)]. Actuators were designed as meandered copper trace resistors R_{act} that warm up via Joule heating when current flows through them ($P_{heat} \propto I^2 R_{act}$). Each actuator consisted of a 4852-mm-long copper trace, laid out over a square area with 74.7-mm sides, resulting in a 9.1-ohm resistance.

Each actuator was powered with 12 V from the system main power supply, and it was individually modulated by the microcontroller via pulse-width modulation. This control signal was sent to a gate driver chip (TI UCC27517A) that enabled fast actuation of a power MOSFET with low R_{ON} (Vishay SiSS12DN) and connected to each thermal actuator (fig. S5A). We numerically implemented a proportional integral differential controller for each actuator's duty cycle, although note that the system can accommodate diverse control strategies.

Mechanical construction

To allow the instrumentation of hives used in science (observation hives) and agriculture (box hives), we designed the robotic system was designed in the form of a Zander beekeeping frame (420 mm by 220 mm; fig. S5B). The frame structure consists of a sandwich of six layers with a printed circuit board (PCB) made of 1.6-mm FR-4 (epoxy and fiberglass) in the center. The PCB is surrounded by six laser-cut layers, where the four outermost layers are made of plexiglass and the two closest to the center are made of 1-mm-thick wood laminate. The wood layers exhibit a hexagonal pattern to serve as a honeycomb construction template for worker bees (Fig. 1), with cells presenting minor and major inner axes of 4.55 and 5.25 mm, respectively. The monitored and actuatable area of the frame has a surface area of 410 mm by 180 mm and is fully covered by the hexagonal mesh. The in-hive atmosphere is very humid, and bees can be very protective against foreign bodies (for example, by chewing soft materials or covering parts with propolis). Therefore, to protect the temperature sensors installed inside cells, we coated them with a 50- to 75-μm acrylic resin layer (MG chemicals 419D), and electronics and connectors were placed inside the protected "electronics bay," in the upper 30 mm of the frame. When designing the elements of the robotic system, including control software, hardware, and materials, we were committed to ethical principles to preserve the animals' welfare, and we considered the consequences of mixing robotic devices and living organisms (see Supplementary Discussion "Ethical considerations").

Robotic system preparation

To prepare the robotic device for experimental colonies' integration, we coated the hexagonal mesh on both sides of the honeycomb with melted beeswax. This structure led to better bio-acceptance and provided initial building material for the construction of honeycombs (Fig. 1). Once prepared, the devices were inserted either into a populated box hive, by replacing one of the nine conventional Zander combs (colonies B and C), or directly into an observation hive with a bee colony (colony A). Robotic systems that were added to established colonies in box hives had fully drawn cells constructed after 10 to 14 days and were then transferred to observation hives. Because there is comparatively less space in an observation colony, hence fewer bees, the construction of the combs took slightly longer there (~21 days). All experiments were made in observation hives in the HFLG at the Botanical Gardens of the University of Graz, in Graz, Austria.

Animals, colonies, and hives

Colonies of *A. mellifera carnica* Pollmann, bred for commercial use by the Styrian Beekeeping Center, Austria, were established at the University of Graz for the purposes of scientific research. According to the principles of animal care of the University of Graz, the ethics commission of the university, and the Austrian Animal Experiments Act (Tierversuchsgesetz 2012-TVG 2012, 1. Abschnitt, §1), no ethical approval is required for experiments with insects. The animals received appropriate care from a professional animal keeper before, during, and after observations and experiments. A queen was introduced to the colony and acclimatized in a queen cage for 3 days before being released to roam freely in the colony. During the entire experimental period, the bees were fed ad libitum with 73% sucrose solution.

Three colonies were used in this study. Colony A was used in the observation and modulation experiments, performed during the 2020–2021 winter season, with an estimated initial size of 4000 bees. The system was installed in the hive on 1 August 2020 where preliminary tests and observational experiments were conducted, accounting for a total of 180 days inside the colony (preliminary and experimental phases). For this colony, the data presented above are from 1 December 2020 to 28 January 2021. Measurements from colonies B and C were taken during the 2021–2022 winter season and presented in the colony collapse and closed-loop experiment results, respectively. These colonies were estimated to have an initial size of 5000 bees.

In the experiments, we used observation hives (width × height × depth = 53 cm × 68 cm × 11 cm) containing two vertically stacked Zander frames. In colonies A and C, we used one robotic system, and in colony B, two were used. Pipes installed in the lower part of the hives gave bees access to the exterior. Both faces of the hives were covered by 4-mm antireflective glass windows (Conturan Magic), allowing the colony activity to be recorded (fig. S5C).

Experimental setup

At the observation hives in the HFLG, each robotic device was controlled by a dedicated single-board computer (SBC; Raspberry Pi 4) located outside the hive. In addition, two extra SBCs controlled four cameras [Raspberry Pi High-Quality Camera, with the 6-mm CS-mount lens with removed infrared (IR) filter] facing the combs from the front and backside. Because bees are not sensitive to IR light, hives were illuminated by 12 IR lamps (Synergy 21 light-emitting diode retrofit 4 × 1 W IR security) equipped with paper diffusers. The dedicated SBC orchestrated the behavior of the connected robotic device (via its MicroPython interface); collected, processed, and stored measurements; logged system events; recorded images; and lastly uploaded the data to a desktop PC (located in the HFLG).

To allow the analysis of the influence of the ambient surrounding the colony during the experiments, we installed a weather station (Ecowitt Eurochron EFWS 2900) near the HFLG. The

relevant variables to this research were the external temperature T_{ext} and the ambient temperature inside the HFLG T_{amb}, measured through a wireless dongle connected to the weather station. Both temperatures were recorded in intervals of 30 min.

Closed-loop experiment

Before the experiment, actuators $TA_{3,1}$ and $TA_{3,2}$ were activated for 3 days to move the colony to the center of the frame. Then, from 9 January 2022 to 26 January 2022, the robotic system installed within colony C operated autonomously. The robotic device was programmed to attract bees to one of the two defined zones comprising four thermal actuators, with maximum combined heat dissipation of 6 W and regulated to 30°C when active. Once the system measured the cluster residency time inside the desired zone to be longer than 12 hours, it deactivated its thermal actuators and activated the actuators of the opposite zone. The robotic system was programmed to estimate the position of the bees on the basis of their thermal signature. This used an isotherm (T_{iso}) to delimit a contour that would represent the cluster's position. After preliminary work with a constant T_{iso} that failed to track the cluster when ambient temperatures (and consequently T_{min}) were warmer than T_{iso}, we designed a simple piecewise-linear function to define T_{iso}. Specifically, T_{iso} adapted to changes in ambient temperature. For T_{min} values below 11.2°C, $T_{iso} \leftarrow 15$°C. For higher values of T_{min}, the isotherm threshold adapted as $T_{iso} \leftarrow 0.92 \cdot T_{min} + 4.7$, after the linear regression between T_{mantle} and T_{amb} (closely related to T_{min}).

Statistical methods

Sample sizes are described in each result section text and in figure legends. A nonparametric kernel density estimator was used to compute probability density distributions for the observation experiment (fig. S2) and the perturbation experiments (figs. S3 and S4). If not indicated otherwise, measurement estimators are stated as the sample median, and after the symbol ±, the uncertainty is expressed by the robust estimator of spread MAD and found by $\mathrm{MAD}\{x_i\} = 1.4826 \cdot \mathrm{median}\{||x_i - \mathrm{median}\{x_i\}||\}$ (*75*). Confidence intervals at the level of 95% represent the uncertainty of the linear regressions presented in Fig. 3. In some noisy time series, we applied a trend filter (for example, Figs. 3A and 5B), and whenever the level of temporal similarity between series was stated, we computed it via a time-lagged Spearman rank correlation (see Supplementary Methods "Trend filtering" and "Time series relationships").

Data analysis

Optical data were sampled at 4-s intervals from both sides of the hives. The collected images were undistorted and contrast-enhanced via a sequence of algorithms. To understand the cluster structuring, images were automatically segmented to identify areas containing bees (through an adaptative background subtraction method) and zones with bees presenting different levels of motility (via dense optical flow). Details of these methods are included in Supplementary Methods "Visual data sampling and processing."

The thermal fields used in the analysis were generated from the linear interpolation of the 64 temperature values provided by the robotic systems' sensor array. For the extraction of the thermodynamics of different regions of the cluster, we sampled the thermal field at the core, mantle, and peripheral positions extracted from the optical analysis (see Supplementary Methods "Thermal data analysis").

Supplementary Materials

This PDF file includes:
Methods
Discussion
Figs. S1 to S5
References (*76–91*)

Other Supplementary Material for this manuscript includes the following:
Movies S1 to S4
Data files S1 to S4
MDAR Reproducibility Checklist

REFERENCES AND NOTES

1. B. Hölldobler, E. O. Wilson, *The Superorganism: The Beauty, Elegance, and Strangeness of Insect Societies* (WW Norton & Company, 2009).
2. R. F. A. Moritz, S. Fuchs, Organization of honeybee colonies: Characteristics and consequences of a superorganism concept. *Apidologie* **29**, 7–21 (1998).
3. T. D. Seeley, The honey bee colony as a superorganism. *Am. Sci.* **77**, 546–553 (1989).
4. T. D. Seeley, P. K. Visscher, T. Schlegel, P. M. Hogan, N. R. Franks, J. A. R. Marshall, Stop signals provide cross inhibition in collective decision-making by honeybee swarms. *Science* **335**, 108–111 (2012).
5. A. Traveset, C. Tur, V. M. Eguíluz, Plant survival and keystone pollinator species in stochastic coextinction models: Role of intrinsic dependence on animal-pollination. *Sci. Rep.* **7**, 6915 (2017).
6. M. S. Nash, J. P. Anderson, W. G. Whitford, Spatial and temporal variability in relative abundance and foraging behavior of subterranean termites in desertified and relatively intact Chihuahuan Desert ecosystems. *Appl. Soil Ecol.* **12**, 149–157 (1999).
7. L. Elizalde, M. Arbetman, X. Arnan, P. Eggleton, I. R. Leal, M. N. Lescano, A. Saez, V. Werenkraut, G. I. Pirk, The ecosystem services provided by social insects: Traits, management tools and knowledge gaps. *Biol. Rev.* **95**, 1418–1441 (2020).
8. V. Patel, N. Pauli, E. Biggs, L. Barbour, B. Boruff, Why bees are critical for achieving sustainable development. *Ambio* **50**, 49–59 (2021).
9. R. Rader, I. Bartomeus, L. A. Garibaldi, M. P. D. Garratt, B. G. Howlett, R. Winfree, S. A. Cunningham, M. M. Mayfield, A. D. Arthur, G. K. S. Andersson, R. Bommarco, C. Brittain, L. G. Carvalheiro, N. P. Chacoff, M. H. Entling, B. Foully, B. M. Freitas, B. Gemmill-Herren, J. Ghazoul, S. R. Griffin, C. L. Gross, L. Herbertsson, F. Herzog, J. Hipólito, S. Jaggar, F. Jauker, A.-M. Klein, D. Kleijn, S. Krishnan, C. Q. Lemos, S. A. M. Lindström, Y. Mandelik, V. M. Monteiro, W. Nelson, L. Nilsson, D. E. Pattemore, N. d. O. Pereira, G. Pisanty, S. G. Potts, M. Reemer, M. Rundlöf, C. S. Sheffield, J. Scheper, C. Schüepp, H. G. Smith, D. A. Stanley, J. C. Stout, H. Szentgyörgyi, H. Taki, C. H. Vergara, B. F. Viana, M. Woyciechowski, Non-bee insects are important contributors to global crop pollination. *Proc. Natl. Acad. Sci. U.S.A.* **113**, 146–151 (2016).
10. A.-M. Klein, B. E. Vaissière, J. H. Cane, I. Steffan-Dewenter, S. A. Cunningham, C. Kremen, T. Tscharntke, Importance of pollinators in changing landscapes for world crops. *Proc. R. Soc. B Biol. Sci.* **274**, 303–313 (2007).
11. WHO, *Guidance on mainstreaming biodiversity for nutrition and health* (World Health Organization, 2020).
12. O. Dangles, J. Casas, Ecosystem services provided by insects for achieving sustainable development goals. *Ecosyst. Serv.* **35**, 109–115 (2019).
13. F. L. W. Ratnieks, N. L. Carreck, Clarity on honey bee collapse? *Science* **327**, 152–153 (2010).
14. D. vanEngelsdorp, J. D. Evans, C. Saegerman, C. Mullin, E. Haubruge, B. K. Nguyen, M. Frazier, J. Frazier, D. Cox-Foster, Y. Chen, R. Underwood, D. R. Tarpy, J. S. Pettis, Colony collapse disorder: A descriptive study. *PLOS ONE* **4**, e6481 (2009).
15. A. Gray, N. Adjlane, A. Arab, A. Ballis, V. Brusbardis, J.-D. Charrière, R. Chlebo, M. F. Coffey, B. Cornelissen, C. Amaro da Costa, B. Dahle, J. Danihlík, M. M. Dražić, G. Evans, M. Fedoriak, I. Forsythe, A. Gajda, D. C. de Graaf, A. Gregorc, I. Ilieva, J. Johannesen, L. Kauko, P. Kristiansen, M. Martikkala, R. Martín-Hernández, C. A. Medina-Flores, F. Mutinelli, S. Patalano, A. Raudmets, G. S. Martin, V. Soroker, J. Stevanovic, A. Uzunov, F. Vejsnaes, A. Williams, M. Zammit-Mangion, R. Brodschneider, Honey bee colony winter loss rates for 35 countries participating in the COLOSS survey for winter 2018–2019, and the effects of a new queen on the risk of colony winter loss. *J. Apic. Res.* **59**, 744–751 (2020).
16. N. Seitz, K. S. Traynor, N. Steinhauer, K. Rennich, M. E. Wilson, J. D. Ellis, R. Rose, D. R. Tarpy, R. R. Sagili, D. M. Caron, K. S. Delaplane, J. Rangel, K. Lee, K. Baylis, J. T. Wilkes, J. A. Skinner, J. S. Pettis, D. vanEngelsdorp, A national survey of managed honey bee 2014–2015 annual colony losses in the USA. *J. Apic. Res.* **54**, 292–304 (2015).
17. R. Van Der Zee, L. Pisa, S. Andonov, R. Brodschneider, J.-D. Charrière, R. Chlebo, M. F. Coffey, K. Crailsheim, B. Dahle, A. Gajda, A. Gray, M. M. Drazic, M. Higes, L. Kauko, A. Kence,

M. Kence, N. Kezic, H. Kiprijanovska, J. Kralj, P. Kristiansen, R. M. Hernandez, F. Mutinelli, B. K. Nguyen, C. Otten, A. Özkırım, S. F. Pernal, M. Peterson, G. Ramsay, V. Santrac, V. Soroker, G. Topolska, A. Uzunov, F. Vejsnæs, S. Wei, S. Wilkins, Managed honey bee colony losses in Canada, China, Europe, Israel and Turkey, for the winters of 2008–9 and 2009–10. *J. Apic. Res.* **51**, 100–114 (2012).

18. T. D. Seeley, *The Wisdom of the Hive: The Social Physiology of Honey Bee Colonies* (Harvard Univ. Press, 1995).
19. M. A. Döke, M. Frazier, C. M. Grozinger, Overwintering honey bees: Biology and management. *Curr. Opin. Insect Sci.* **10**, 185–193 (2015).
20. H. R. Mattila, J. L. Harris, G. W. Otis, Timing of production of winter bees in honey bee (*Apis mellifera*) colonies. *Insectes Soc.* **48**, 88–93 (2001).
21. J. Krause, A. F. T. Winfield, J.-L. Deneubourg, Interactive robots in experimental biology. *Trends Ecol. Evol.* **26**, 369–375 (2011).
22. G. L. Patricelli, Use of Robotics in the Study of Animal Behavior, in *Encyclopedia of Animal Behavior (Second Edition)*, J. C. Choe, Ed. (Academic Press, 2019), pp. 535–545.
23. D. Romano, E. Donati, G. Benelli, C. Stefanini, A review on animal–robot interaction: From bio-hybrid organisms to mixed societies. *Biol. Cybern.* **113**, 201–225 (2019).
24. T. Landgraf, G. H. W. Gebhardt, D. Bierbach, P. Romanczuk, L. Musiolek, V. V. Hafner, J. Krause, Animal-in-the-loop: Using interactive robotic conspecifics to study social behavior in animal groups. *Annu. Rev. Control Robot. Auton. Syst.* **4**, 487–507 (2021).
25. S. Agrawal, S. Safarik, M. H. Dickinson, The relative roles of vision and chemosensation in mate recognition of *Drosophila melanogaster*. *J. Exp. Biol.* **217**, 2796–2805 (2014).
26. H. Ishii, M. Ogura, S. Kurisu, A. Komura, A. Takanishi, N. Iida, H. Kimura, Experimental Study on Task Teaching to Real Rats Through Interaction with a Robotic Rat, in *From Animals to Animats 9*, S. Nolfi, G. Baldassarre, R. Calabretta, J. C. T. Hallam, D. Marocco, J.-A. Meyer, O. Miglino, D. Parisi, Eds. (Springer Berlin Heidelberg, Berlin, Heidelberg, 2006), vol. 4095 of *Lecture Notes in Computer Science*, pp. 643–654.
27. F. Patane, V. Mattoli, C. Laschi, B. Mazzolai, P. Dario, H. Ishii, A. Takanishi, Biomechatronic Design and Development of a Legged Rat Robot, in *2007 IEEE International Conference on Robotics and Biomimetics (ROBIO)* (IEEE, Sanya, 2007), pp. 847–852.
28. R. Vaughan, N. Sumpter, J. Henderson, A. Frost, S. Cameron, Experiments in automatic flock control. *Robot. Auton. Syst.* **31**, 109–117 (2000).
29. D. T. Swain, I. D. Couzin, N. Ehrich Leonard, Real-time feedback-controlled robotic fish for behavioral experiments with fish schools. *Proc. IEEE* **100**, 150–163 (2012).
30. J. Halloy, G. Sempo, G. Caprari, C. Rivault, M. Asadpour, F. Tache, I. Said, V. Durier, S. Canonge, J. M. Ame, C. Detrain, N. Correll, A. Martinoli, F. Mondada, R. Siegwart, J. L. Deneubourg, Social integration of robots into groups of cockroaches to control self-organized choices. *Science* **318**, 1155–1158 (2007).
31. F. Mondada, J. Halloy, A. Martinoli, N. Correll, A. Gribovskiy, G. Sempo, R. Siegwart, J.-L. Deneubourg, A General Methodology for the Control of Mixed Natural-Artificial Societies, in *Handbook of Collective Robotics*, S. Kernbach, Ed. (Pan Stanford, 2013;www.crcnetbase.com/doi/10.1201/b14908-19), pp. 547–586.
32. L. T. Reaney, R. A. Sims, S. W. M. Sims, M. D. Jennions, P. R. Y. Backwell, Experiments with robots explain synchronized courtship in fiddler crabs. *Curr. Biol.* **18**, R62–R63 (2008).
33. S. Camazine, J.-L. Deneubourg, N. R. Franks, J. Sneyd, G. Theraula, E. Bonabeau, *Self-organization in Biological Systems* (Princeton University Press, 2003).
34. J. B. Free, Y. Spencer-Booth, Chill-coma and cold death temperatures of Apis Mellifera. *Entomol. Exp. Appl.* **3**, 222–230 (1960).
35. B. Heinrich, Social Thermoregulation, *in The hot-blooded insects: Strategies and mechanisms of thermoregulation* (Springer-Verlag Berlin Heidelberg, 1993).
36. H. Esch, The effects of temperature on flight muscle potentials in honeybees and cuculiinid winter moths. *J. Exp. Biol.* **135**, 109–117 (1988).
37. J. Lecomte, Sur le déterminisme de la formation de la grappe chez les abeilles. *Z. Vgl. Physiol.* **32**, 499–506 (1950).
38. M. Szopek, T. Schmickl, R. Thenius, G. Radspieler, K. Crailsheim, Dynamics of collective decision making of honeybees in complex temperature fields. *PLOS ONE* **8**, e76250 (2013).
39. J. C. Jones, M. R. Myerscough, S. Graham, B. P. Oldroyd, Honey bee nest thermoregulation: Diversity promotes stability. *Science* **305**, 402–404 (2004).
40. B. Bujok, M. Kleinhenz, S. Fuchs, J. Tautz, Hot spots in the bee hive. *Naturwissenschaften* **89**, 299–301 (2002).
41. S. Kühnholz, T. D. Seeley, The control of water collection in honey bee colonies. *Behav. Ecol. Sociobiol.* **41**, 407–422 (1997).
42. C. N. Cook, S. Durzi, K. J. Scheckel, M. D. Breed, Larvae influence thermoregulatory fanning behavior in honeybees (*Apis mellifera* L.). *Insectes Soc.* **63**, 271–278 (2016).
43. R. E. Bonoan, R. R. Goldman, P. Y. Wong, P. T. Starks, Vasculature of the hive: Heat dissipation in the honey bee (*Apis mellifera*) hive. *Naturwissenschaften* **101**, 459–465 (2014).
44. A. Stabentheiner, H. Pressl, T. Papst, N. Hrassnigg, K. Crailsheim, Endothermic heat production in honeybee winter clusters. *J. Exp. Biol.* **206**, 353–358 (2003).
45. E. E. Southwick, Metabolic energy of intact honey bee colonies. *Comp. Biochem. Physiol. A Physiol.* **71**, 277–281 (1982).
46. K. Griparic, T. Haus, D. Miklic, S. Bogdan, Combined Actuator Sensor Unit for Interaction with Honeybees, *in 2015 IEEE Sensors Applications Symposium (SAS)* (IEEE, Zadar, 2015), pp. 1–5.
47. M. Stefanec, M. Szopek, T. Schmickl, R. Mills, Governing the Swarm: Controlling a Bio-Hybrid Society of Bees Robots with Computational Feedback Loops, in *2017 IEEE Symposium Series on Computational Intelligence (SSCI)* (2017), pp. 1–8.
48. T. Schmickl, M. Szopek, F. Mondada, R. Mills, M. Stefanec, D. N. Hofstadler, D. Lazic, R. Barmak, F. Bonnet, P. Zahadat, Social integrating robots suggest mitigation strategies for ecosystem decay. *Front. Bioeng. Biotechnol.* **9**, 612605 (2021).
49. C. D. Owens, *The Thermology of Wintering Honey Bee Colonies* (U.S. Agricultural Research Service, 1971).
50. E. E. Southwick, Overwintering in Honey Bees: Implications for Apiculture, in *Insects at Low Temperature*, R. E. Lee, D. L. Denlinger, Eds. (Springer US, 1991), pp. 446–460.
51. T. S. K. Johansson, M. P. Johansson, The honeybee colony in winter. *Bee World* **60**, 155–170 (1979).
52. B. Kraus, H. H. W. Velthuis, S. Tingek, Temperature profiles of the brood nests of *Apis cerana* and *Apis mellifera* colonies and their relation to varroosis. *J. Apic. Res.* **37**, 175–181 (1998).
53. D. Severson, E. Erickson Jr., Quantification of cluster size and low ambient temperature relationships in the honey bee. *Apidologie* **21**, 135–142 (1990).
54. T. I. Szabo, The thermology of wintering honeybee colonies in 4-colony packs as affected by various hive entrances. *J. Apic. Res.* **24**, 27–37 (1985).
55. E. E. Southwick, G. Heldmaier, Temperature control in honey bee colonies. *Bioscience* **37**, 395–399 (1987).
56. J. R. Harbo, Effect of population size on worker survival and honey loss in broodless colonies of honey bees, *Apis mellifera* L. (Hymenoptera: Apidae). *Environ. Entomol.* **12**, 1559–1563 (1983).
57. W. G. Meikle, N. Holst, Application of continuous monitoring of honeybee colonies. *Apidologie* **46**, 10–22 (2015).
58. G. Retschnig, G. R. Williams, R. Odemer, J. Boltin, C. Di Poto, M. M. Mehmann, P. Retschnig, P. Winiger, P. Rosenkranz, P. Neumann, Effects, but no interactions, of ubiquitous pesticide and parasite stressors on honey bee (*Apis mellifera*) lifespan and behaviour in a colony environment. *Environ. Microbiol.* **17**, 4322–4331 (2015).
59. T. D. Seeley, Temperature control, in *The Lives of Bees: The Untold Story of the Honey Bee in the Wild* (Princeton Univ. Press, 2019).
60. E. Rademacher, M. Harz, S. Schneider, Effects of oxalic acid on *Apis mellifera* (Hymenoptera: Apidae). *Insects* **8**, 84 (2017).
61. M. R. Myerscough, A simple model for temperature regulation in honeybee swarms. *J. Theor. Biol.* **162**, 381–393 (1993).
62. J. Watmough, S. Camazine, Self-organized thermoregulation of honeybee clusters. *J. Theor. Biol.* **176**, 391–402 (1995).
63. D. J. T. Sumpter, D. S. Broomhead, Shape and dynamics of thermoregulating honey bee clusters. *J. Theor. Biol.* **204**, 1–14 (2000).
64. S. A. Ocko, L. Mahadevan, Collective thermoregulation in bee clusters. *J. R. Soc. Interface* **11**, 20131033 (2014).
65. R. Bastiaansen, A. Doelman, F. van Langevelde, V. Rottschäfer, Modeling honey bee colonies in winter using a keller-segel model with a sign-changing chemotactic coefficient. *SIAM J. Appl. Math.* **80**, 839–863 (2020).
66. B. Heinrich, Energetics of honeybee swarm thermoregulation. *Science* **212**, 565–566 (1981).
67. A. Stabentheiner, H. Kovac, M. Mandl, H. Käfer, Coping with the cold and fighting the heat: Thermal homeostasis of a superorganism, the honeybee colony. *J. Comp. Physiol. A Neuroethol. Sens. Neural Behav. Physiol.* **207**, 337–351 (2021).
68. I. Nolasco, A. Terenzi, S. Cecchi, S. Orcioni, H. L. Bear, E. Benetos, Audio-based Identification of Beehive States, in *ICASSP 2019–2019 IEEE International Conference on Acoustics, Speech and Signal Processing (ICASSP)* (IEEE, 2019), pp. 8256–8260.
69. A. Szczurek, M. Maciejewska, B. Bąk, J. Wilde, M. Siuda, Semiconductor gas sensor as a detector of *Varroa destructor* infestation of honey bee colonies – Statistical evaluation. *Comput. Electron. Agric.* **162**, 405–411 (2019).
70. Y. Le Conte, G. Arnold, P. Desenfant, Influence of brood temperature and hygrometry variations on the development of the honey bee Ectoparasite *Varroa jacobsoni* (Mesostigmata: varroidae). *Environ. Entomol.* **19**, 1780–1785 (1990).
71. K. Bozek, L. Hebert, Y. Portugal, A. S. Mikheyev, G. J. Stephens, Markerless tracking of an entire honey bee colony. *Nat. Commun.* **12**, 1733 (2021).
72. D. Mitchell, Ratios of colony mass to thermal conductance of tree and man-made nest enclosures of *Apis mellifera*: Implications for survival, clustering, humidity regulation and *Varroa destructor*. *Int. J. Biometeorol.* **60**, 629–638 (2016).

73. F. Kronenberg, H. C. Heller, Colonial thermoregulation in honey bees (*Apis mellifera*). *J. Comp. Physiol.* **148**, 65–76 (1982).
74. G. W. Otis, Weights of worker honeybees in swarms. *J. Apic. Res.* **21**, 88–92 (1982).
75. P. J. Rousseeuw, Tutorial to robust statistics. *J. Chemometrics* **5**, 1–20 (1991).
76. E. E. Southwick, D. Pimentel, Energy efficiency of honey production by bees. *Bioscience* **31**, 730–732 (1981).
77. A. Ramdas, R. J. Tibshirani, Fast and flexible ADMM algorithms for trend filtering. *J. Comput. Graph. Stat.* **25**, 839–858 (2016).
78. R. J. Tibshirani, Adaptive piecewise polynomial estimation via trend filtering. *Ann. Stat.* **42**, 285–323 (2014).
79. B. Bruder, T.-L. Dao, J.-C. Richard, T. Roncalli, trend filtering methods for momentum strategies. *SSRN Electron. J.* , (2011).
80. G. Farnebäck, Two-Frame Motion Estimation Based on Polynomial Expansion, in *Image Analysis*, J. Bigun, T. Gustavsson, Eds. (Springer, 2003), *Lecture Notes in Computer Science*, pp. 363–370.
81. Z. Zivkovic, Improved adaptive Gaussian mixture model for background subtraction, in *Proceedings of the 17th International Conference on Pattern Recognition, 2004. ICPR 2004.* (2004), vol. 2, pp. 28–31.
82. S. Suzuki, K. Be, Topological structural analysis of digitized binary images by border following. *Comput. Vis. Graph. Image Process.* **30**, 32–46 (1985).
83. P. J. Rousseeuw, M. Hubert, Anomaly detection by robust statistics. *WIREs Data Min. Knowl. Discov.* **8**, e1236 (2018).
84. A. J. Ijspeert, Biorobotics: Using robots to emulate and investigate agile locomotion. *Science* **346**, 196–203 (2014).
85. N. W. Xu, J. O. Dabiri, Low-power microelectronics embedded in live jellyfish enhance propulsion. *Sci. Adv.* **6**, eaaz3194 (2020).
86. T. T. Vo Doan, M. Y. W. Tan, X. H. Bui, H. Sato, An ultralightweight and living legged robot. *Soft Robot.* **5**, 17–23 (2018).
87. J. Donhauser, A. van Wynsberghe, A. Bearden, Steps toward an ethics of environmental robotics. *Philos. Technol.* **34**, 507–524 (2021).
88. D. Grémillet, W. Puech, V. Garçon, T. Boulinier, Y. L. Maho, Robots in ecology: Welcome to the machine. *Open J. Ecol.* **02**, 49–57 (2012).
89. I. L. Mason, *Evolution of Domesticated Animals* (Longman, 1984), pp. 403–415.
90. M. D. Meixner, C. Costa, P. Kryger, F. Hatjina, M. Bouga, E. Ivanova, R. Büchler, Conserving diversity and vitality for honey bee breeding. *J. Apic. Res.* **49**, 85–92 (2010).
91. D. W. Scott, *Multivariate Density Estimation: Theory, Practice, and Visualization* (John Wiley & Sons, 1992).

Acknowledgments: We thank D. Burnier and N. Crot for suggestions on mechanical and electronic design and the Botanical Gardens at the University of Graz for hosting the honeybees. **Funding:** This work was supported by the EU H2020 FET project HIVEOPOLIS (no. 824069) and by the Field of Excellence COLIBRI (Complexity of Life in basic Research and Innovation) at the University of Graz. **Author contributions:** Conceptualization: R.B., M.S., D.N.H., F.M., T.S., and R.M. Data curation: R.B., D.N.H., and R.M. Methodology: R.B., M.S., D.N.H., L.P., S.S.-F.S., F.M., T.S., and R.M. Investigation: R.B., M.S., D.N.H., T.S., and R.M. Formal analysis: R.B., M.S., D.N.H., and R.M. Visualization: R.B. and D.N.H. Software: R.B., D.N.H., L.P., and R.M. Writing—original draft: R.B., M.S., D.N.H., T.S., and R.M. Writing—review and editing: R.B., M.S., D.N.H., L.P., S.S.-F.S., F.M., T.S., and R.M. **Competing interests:** The authors declare that they have no competing interests. **Data and materials availability:** All data needed to evaluate the conclusions in the paper are present in the paper or the Supplementary Materials. The data and the software for this study have been deposited in the Zenodo database at https://doi.org/10.5281/zenodo.7671163 (data) and https://doi.org/10.5281/zenodo.7671291 (software).

Submitted 1 July 2022
Resubmitted 23 December 2022
Accepted 28 February 2023
Published 22 March 2023
10.1126/scirobotics.add7385

Science Robotics

A robotic honeycomb for interaction with a honeybee colony

Rafael Barmak, Martin Stefanec, Daniel N. Hofstadler, Louis Piotet, Stefan Schönwetter-Fuchs-Schistek, Francesco Mondada, Thomas Schmickl, and Rob Mills

Sci. Robot. **8** (76), eadd7385. DOI: 10.1126/scirobotics.add7385

Science Robotics (ISSN 2470-9476) is published by the American Association for the Advancement of Science. 1200 New York Avenue NW, Washington, DC 20005. The title *Science Robotics* is a registered trademark of AAAS.